POLITECNICO DI TORINO

Master's Degree in Biomedical Engineering

Estimation of Muscles fatigue by ions and EMG sensors

Master's Degree Thesis

Supervisor

Prof. Sandro CARRARA

Prof. Danilo DEMARCHI

Candidate

Giuliano Angelo GIUFRÈ

July 2021

I

Summary

There is growing interest in health monitoring using non invasive wearable devices. Clinics often use blood analysis for the monitoring condition of the human body but it often requires invasive and annoying collection and is not suitable for continuous monitoring. In order to solve these issues, sweat has recently been deeply studied by researchers and identified as a potential blood substitute in diagnosis. Metabolic markers that are present in sweat, indeed, could provide a more direct indicator of human health for accurate assessment of athletic performance, clinical diagnosis, and for managing chronic health conditions including generating alerts in cases of emergencies. Sweat is promising since it is easily accessible and can be collected non invasively using the iontophoresis or chemical stimulation methods. Sweat is very rich in physiological and metabolic biomarkers, for example, sodium from sweat can indicate the hydration status and electrolyte imbalance in a body, lactate concentration can be an indicator of the muscle fatigue, ammonium for metabolic conditions, potassium level for muscle cramps dehydration and cardiovascular problem and calcium for the bone mineral loss. Among all biomarkers, potassium, sodium, calcium and ammonium have been investigated in this work with the purpose of establishing a quantitative measure of muscle fatigue. All solid-state potentiometric ion-selective electrodes have been explored and applied, since they provide the necessary characteristics suitable for miniaturization and for wearable applications. In order to have a term of comparison for the muscle fatigue the surface EMG signals of the lower limb have been analyse. For these reasons a cycling experimental protocol based on a graded load exercise have been implemented to induce progressively muscle fatigue during which both ions concentration in sweat and EMG are measured.

Table of Contents

List of Tables

List of Figures

Acronyms

CE Counter Electrode

CP Conductive Polymers

CV Cyclic Voltametry

DC Direct current

EMG Electomyography

FFM Fixed interference method

ISE Ion-Selective Electrode

ISM Ion-Selective-Membrane

IUPAC International Union of Pure and Applied Chemistry

LOD Limit of detection

MF Median frequency

OCP Open circuit potential

PVC Polyvinyl Chloride

RE Reference Electrode

RMS Root mean square

SC Solid Contact

SPE Screen printed electrode

SSM Separate solution method

SC-ISE Solid-Contact Ion-Selective Electrode

THF Tetrahydrofuran

WE Working Electrode

Chapter 1

Introduction

This thesis proposes some efficient solutions for handling and processing of the biological information present in sweat, one of the most promising bodily fluid as a non-invasive alternative to blood. Sweat offers some exclusive promising characteristics. In fact, it is readily accessible and reproducible in the laboratory, it does not require invasive procedures, it contains several recognized biomarkers (electrolytes and metabolites) with diagnostic capabilities and good correlation with blood values, and it can be easily monitored continuously [1, 2].
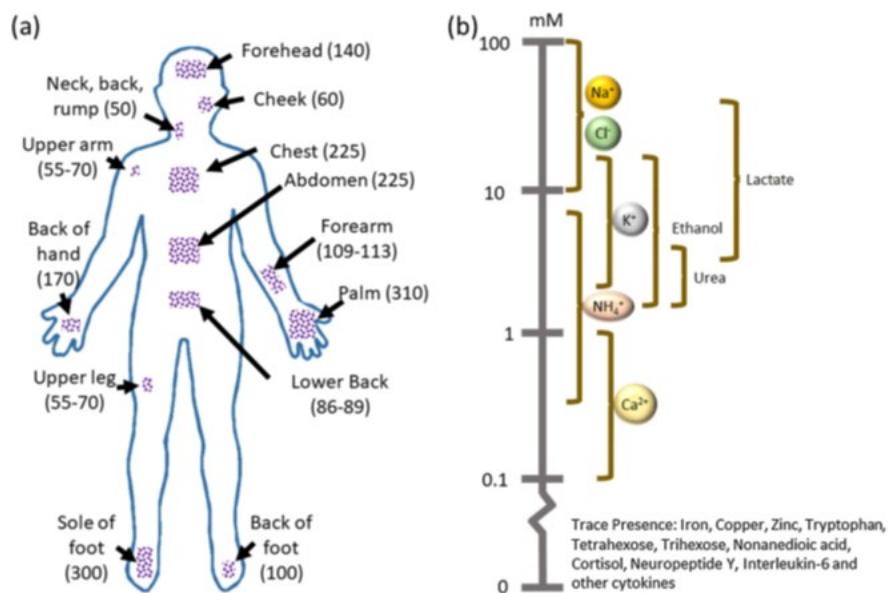
Figure 1.1: a) Distribution of eccrine sweat glands in the human body (glands/CM2). b) Concentration ranges of different sweat analytes.[3]

1.1 Alternative bodily fluids

Blood serum analysis is considered the gold standard for measuring chemical compounds concentration. However, most medical tests require qualified personal and are impractical for continuous monitoring. Therefore, significant interest has shifted to the already mentioned sweat, saliva, tears and interstitial fluid. Each biofluid poses major limitations with respect the sweat. On-demand and continuous monitoring of tears is critical due to eye irritatation caused by the cuurent sample collection protocols and stimulate the production of reflex tears that interfere with the readings. Saliva monitoring is challenging as the chemical composition depends heavily on food or drink eaten by peoples. Furthermore, plaques and bacteria contained in food particles could compromise sensor surfaces. Finally, interstitial fluid requires the use of fine microneedles or subcutaneous excitation currents to collect samples which can be irritating to dermal tissue especially during prolonged monitoring.[3].

1.2 Eccrine sweat glands

There are primarily two types of sweat glands: apocrine and eccrine. The second ones are present in larger number, with higher concentration under the feet, in the palms and in the forehead. The distribution of eccrine sweat gland in the human body is reported in Figure 1.1 [3]. Eccrine sweat is typically composed of water mixed with products originating from the blood, such as urea, sodium chloride, immunoglobulins and proteins. It is odorless. On the contrary apocrine sweat glands are typically located within hair follicles in private areas of the human body. They can activate with stress, emotions or high levels of adrenaline [3]. The sweat produced by eccrine glands is the one of interest for wearable applications so it is worthwhile to understand the anatomy and the method of natural production of sweat.

Each eccrine gland consists of a secretory spiral and a dermal duct (Fig. 1.2a-b). The secretory spiral is located inside the dermal layer of the skin and attracts water to counteract the osmotic gradient generated by the sodium and chloride ions that are actively transported within it. The hydrostatic pressure allows the passage of the fluid up to the surface of the skin through the dermal duct and the secretory coil. During this step various species such as hormones, ions, metabolites and proteins begin to enter into sweat (Fig. 1.2c). Most of these chemical species arise from the active or passive transport of interstitial fluid or nearby blood vessels. This would explain the commonalities in the analytes found in sweat, interstitial fluid, and blood.
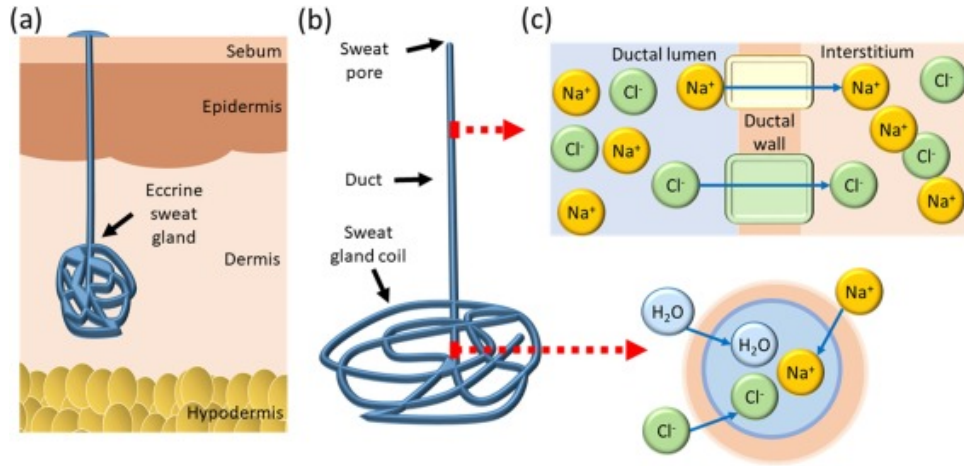
Figure 1.2: Production of sweat from eccrine sweat glands. (a) Skin structure around a sweat gland. (b) Anatomy of a sweat gland. (c) Ionic flow in the ductal and coil regions of a sweat gland. [3]

1.3 Application area

Sweat contains in general electrolytes (i.e. sodium, potassium, magnesium, chloride, calcium),organic compounds (e.g. urea, ammonia, ethanol, lactate), metabolites and trace compounds (e.g. zinc, iron, tryptophan, interleukin 6). The typical concentration rate in sweat are reported in Figure 1.1b [3]. A lot of research is currently going on sweat test as a potential candidate to substitute blood analysis [1, 4, 5]. In fact, the academic publishing has more than quadrupled publications in this area over the past 10 years (Figure 1.3). Electrochemistry is the most investigated sensing method because of the good sensitivity, small sample volume, low cost, simple design, easy integration into microfabrication processes for large-scale production and straightforward signal interpretation. Sweat biomarkers can be used to detect some diseases or the genetic predisposition to diseases. The level of chlorides is useful to determine cystic fibrosis or other related conditions. Furthermore, continuous monitoring of diabetes is possible by measuring the concentration of glucose in sweat, indeed recently studied confirmed the correlation between sweat glucose with blood values. Lactate and ammonia can be an indicator of muscle fatigue [6] and Ischemia. Sodium and potassium can indicate the hydration status and electrolyte imbalance in a body [7]. Urea and creatinine might indicate renal dysfunction. Iron and copper concentration might be used to monitor sports anemia [3, 8].
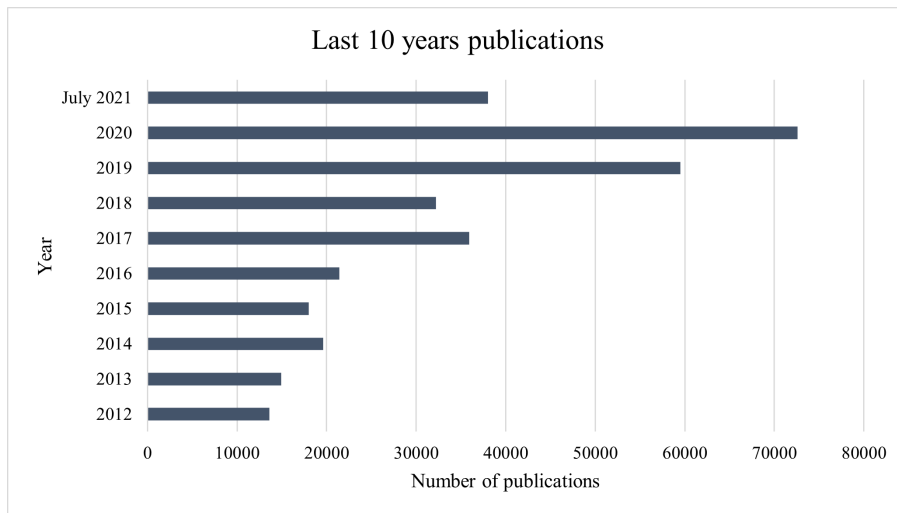
Figure 1.3: Scientific papers published in the past 10 years regarding sweat sensors.

However, the concentration ranges can change significantly under different conditions [9], for example: dietary factors, where diets are low in specific electrolytes can lead to a significant loss of ions during exercise; thermal stress, an unacclimated individual could suffer from greater electrolyte losses; environmental conditions, in which humidity and temperature influences the sweating rate of the individual; sex, electrolyte concentration may differ between males and females; regional sweating rates, the rates are different depending on the region of the body, leading to fluctuations in electrolyte levels; hydration state of the body, dehydration, overhydration or dehydration affects the electrolyte losses; and the intensity of the exercise, due to thermoregulation response to sweating, the threshold for vasodilation is different from one region of the body to another as well as between individuals [10]. Consequently, the (linear) working range of the sweat sensor must be larger enough to succeeding in coping with the concentration ranges found on the skin, thereby providing information relevant to health care and sports performance monitoring. However, ion sensors find application in several different fields outside healthcare, like food and water quality monitoring, industrial control, agriculture and fishery. The same technology developed in this work might be easily extended to other functions outside medical care. In this work the detection of ions is based on the use of ISEs. Their structure and functioning will be illustrated in detail in Chapter 2. ISEs represent the largest part of current ion sensors. This can be explained by considering that fast and non-expensive measurements are possible with these devices. In addition, low maintenance is needed.

1.4   Project contributions

Creating a fully integrated system for measuring sweat analytes remains complex. This type of biosensors still has to face several unsolved problems, such as poor collection, separation sampling and analysis, poor multisensory skills and lack of data correlating sweat and blood values. Advances in materials science to improve selectivity, detection range e stability is also needed. This thesis tries to solve some of these problems, focusing mainly on the detection of ions in sweat to look for a quantitative measure of muscle fatigue. In fact, the concentration of cations in sweat such as potassium, sodium, calcium and ammonium is closely linked to physical activity and in particular to muscle fatigue (Table 1.1). Indeed, nowadays it is not possible to have a measurement of muscle fatigue with a wearable sensor that is not based on the measurement of the EMG signal. This involves the use of sensors and electrodes connected to the affected muscles which makes difficult a simple, comfortable and economical use.

	Range (mM)	Biomarker for physiology	Biomarker for medical condition
Potassium	1-24	Muscle activity	Hypo-or hyperkalemia
Sodium	1-100	Dehydration	Cystic fibrosis
Calcium	0.41-12.4	Homeostasis, stress fractures	Hyperparathyroidism and kidney-stone
Ammonium	0.1-8	Muscle fatigue	Liver dysfunction

Table 1.1: Ranges of ions concentration in sweat and role in human body

1.5   Thesis outline

The outline of the thesis is reported below.

- Chapter 1: Potential of sweat sensing and related application areas.

- Chapter 2 : Detailed background on the basic principles and applications of potentiometric ion-sensors, with particular focus on the effort to develop all-solid-state ISEs.

- Chapter 3 : Procedures and techniques used in this work for the realization and characterization of the sensors.

- Chapter 4 : Obtained results in water and artificial sweat.

- Chapter 5 : Cycling experimental protocol developed as term of comparison for muscle fatigue and EMG signals analysis.

- Chapter 6 : Brief summary of the main achievements of this work and some insights for future works.

Chapter 2

Ion-Selective Electrodes (ISEs)

This chapter gives some background on the basic principles and applications of potentiometric ion-sensors. Ion Selective Electrodes (ISEs) are known as membrane electrodes responding carefully to ions, in the presence of others. These systems exploit Ion-Selective Membranes (ISMs) to efficiently detect the target ion in solution by means of Open Circuit Potential (OCP) measurements. They are widely used for several applications thanks to their high accuracy and simple detection principle [11]. However, conventional ISEs are based on bulky liquid-junctions. Consequently, the research has tried in the last decades to create efficient and miniaturized all-solid-state ISEs, suitable for portable and wearable applications.
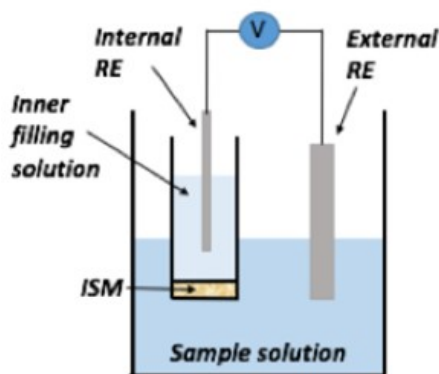
Figure 2.1: Electrochemical setup for potentiometricmeasurements using conventional ISEs [11]

All ISEs are based on the deposition on the sensor surface of an ISM that contains a species, called ionophore, that selectively binds to the target ion. Higher ion concentrations in solution will result in larger amounts of ions in the ISM. This produces a measurable and proportional Open Circuit Potential with respect to a stable Reference Electrode (RE).

2.1 Conventional ISE

The structure and working principle of conventional ISE is shown in Figure 2.2. It can be observed that they are macroscopic systems. An ISM is used to separate an inner filling solution with constant Cl^- concentration from the sample solution [12, 13]. The ISM allows the flow and entrapment of only one specific ion through it. Such selectivity of the ISM is ensured by the presence of an ionophore, that is a neutral species that selectively binds to the target ion M^+. Typical membrane cocktails include 1-2% of ionophore, 60-70% of plasticizer and 30-40% of high molecular weight PolyVinyl Chloride (PVC). The polymeric matrix gives mechanical stability and should be chemically inert. The plasticizer increases the free volume of the polymeric materials, thus improving mobility, flexibility and durability. Commonly used plasticizers are bis(2-ethylhexyl)sebacate (DOS) or ortho-nitrophenyl octyl ether (o-NPOE). In order to ensure Nernstian behaviour, small amounts of lipophilic ions are added to avoid the extraction of a large amount of counterions from the sample solution to the ISM [11, 14, 15]. For a conventional ISE, the inner reference electrode is often composed of a AgCl coated Ag wire, in contact with an inner filling solution containing Cl^- with a constant concentration (Figure 2.2).
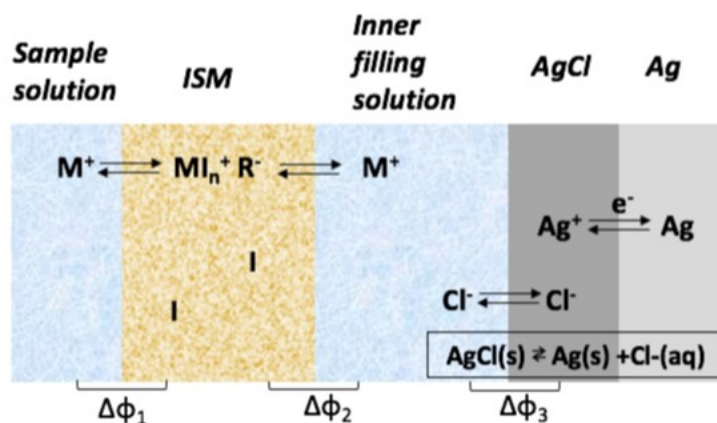
Figure 2.2: Structure and working principle of conventional ISEs. [11]

If the concentrations of the ions in the inner and the sample solution are not equal, then a potential difference is generated across the membrane due to ions exchange and accumulation in the ISM. It is possible to predict the activity of the target ion in solution by measuring the OCP of this kind of Working Electrode (WE) with respect to a stable RE. In particular, by keeping constant the activity of the target ion in the internal solution a_A, Nernst equation can be employed to determine the unknown activity on the other side of the membrane a_x :

$$E = \frac{RT}{z_a F} In(\frac{a_x}{a_A}) = cost + 2.3\frac{RT}{z_a F} log a_x \tag{2.1}$$

where R is the general gas constant, T the temperature, z_A the valence of the target ion and F Faraday's constant. The internal filling solution acts as a liquid contact that ensures ionto-electron transduction thanks to the reaction $AgCl(s) \rightarrow Ag(s) + Cl^-(aq)$ and consequent definition of the interfacial potential $\Delta\phi_3$. It is important to notice that ISEs can detect free, not complex, ion concentrations [11, 16]. The slope of the calibration curve is $\frac{RT}{z_a F}$, and represents the sensitivity of the sensor S. By simple calculations, it is possible to prove that S = $59.16/z_A$ at ambient temperature. The sensitivity of potentiometric sensor is mainly dependent on the ions charge z. Monovalent cations will have a calibration slope of 59 mV/decade, which means that a 10-fold concentration will cause a change of 59 mV in the measured potential. On the contrary, the divalent cations will generate a calibration curve with a slope of 29.6 mV/decade.

2.2   Towards all solid-state ISEs

Conventional ISEs are very accurate, with small potential drift and long lifetime. However, they have several limits that must be overcome for the realization of portable and wearable devices [14]. This problem is mainly due to the liquid contact (referred to as inner filling solutions) between the membrane and the internal reference. In particular this liquid contact makes the sensor sensitive to:

- Evaporation of the inner filling solution.

- Changes in sample temperature and preassure.

- Osmotic pressure wich can lead to a large volume changes and delamination of the sensing membrane.

Thus, it is highly desirable to eliminate the cumbersome liquid contacts by replacing conventional electrodes with all-solid-state potentiometric sensors. In all-solid-state ISEs and reference electrodes, a solid contact is formed between the sensing membrane and an electron-conducting substrate to replace the liquid contact, also

serving as an ion-to-electron transducer. The two types of solid-contact(SC) that are actually used in the ISM applications are conductive polymers and nanostructures with high double layer capacitance. In the following paragraphs, we will discuss the advantages and drawbacks of each system.

2.2.1 Conductive Polymers (CPs)

Considering their capability to conduct efficiently electrons and ions, conductive polymers are commonly used as solid contacts in ISEs applications. However, they could play the role of ion-to-electrons transducers by redox reactions(Figure 2.3).
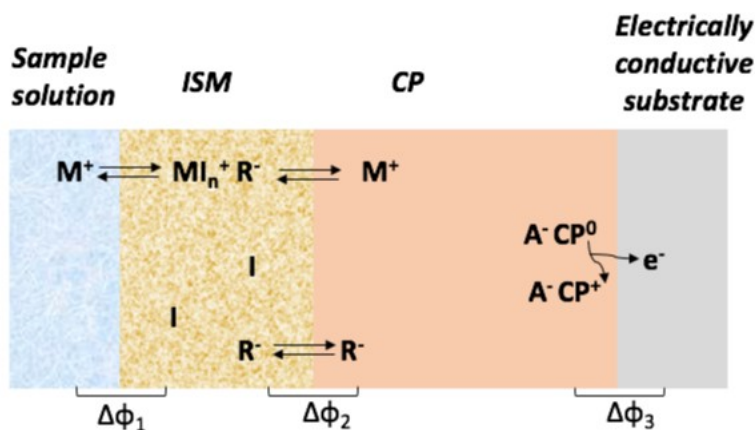
Figure 2.3: Structure and working principle of SC-ISEs, based on CPs [11]

Common materials that have been used, to characterize the conductive polymers as solidcontacts for the ISEs, are Polypyrrole [[11], poly(3,4-ethylenedioxytiophene (PEDOT) [17], polyaniline [11], and poly(3-octyltiophene) (POT) [18]. They are obtained, either by electropolymerization deposition, or drop casting from polymeric solutions. Polypyrrole, PEDOT and POT are extremely stable and able to provide large conductivity and redox capacitance against multiple side reactions and non-negligible drift in a large potentials range, due to their electro-activity. On the other hand, POT causes much less side reactions against much lower conductivity and redox capacitance [11].

2.2.2 Nanostructured Materials

Nanostructured materials exploit the formation of an electrical double layer at the membrane/electrode interface for ion-to-electron transduction. This happens because the membrane favors the accumulation of ions on one side of the interface and holes on the other. This creates an asymmetric capacitor. In these systems the

interfacial potential is not related to redox reactions, as in the case of conductive polymers, or to ion partitioning, as in conventional ISEs, but to the amount of charge accumulated in the double layer, leading to the potential different $\Delta\phi_2$ (Figure 2.4).
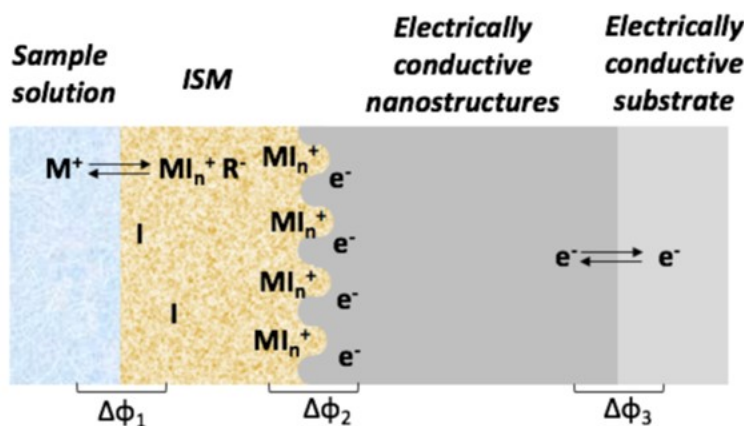
Figure 2.4: Structure and working principle of SC-ISEs, based on based on nanostructures with high double layer capacitance [11]

The most crucial and common issues of all-solid-state ISEs is potential drift over a long period of time, i.e. potential instability. This is typically due to the formation of a water layer at the ISM/SC interface. Its formation can be deducted from several effects: slow stabilization time, sensitivity of the sensor to osmolality variations, positive potential drift upon addition of interfering ions, negative drift upon their elimination. However, Nanostructured materials offer several advantages with respect CPs. Thanks to their large surface area, enable to avoid the risk of water absorption, and are typically characterized by high capacitance values. This property is crucial to reduce polarization effects due to the small but non-zero currents required for the measurement. As well as having the ability to achieve high conductivity, the absence of possible side-reactions and the insensitivity to pH and light. Potential stability can be measured by reverse current chronopotentiometry (CRC). The method allows to verify the potential drift by applying a current of a few nanoamperes, which is then inverted. In this way the slope of the curve will be indicative of the potential stability. Criscuolo et al. [19] performed these measurements on a Li^+ SC-ISE with and without the presence of gold and platinum nanostructures. As can be seen in the figure 2.5, the presence of nanostructures in both cases greatly improves the potential stability compared to the deposition of the membrane directly on the SPE. This improvement can be attributed to the different ion-to electron transduction mechanism that is exploited by nanostructured

10

materials.
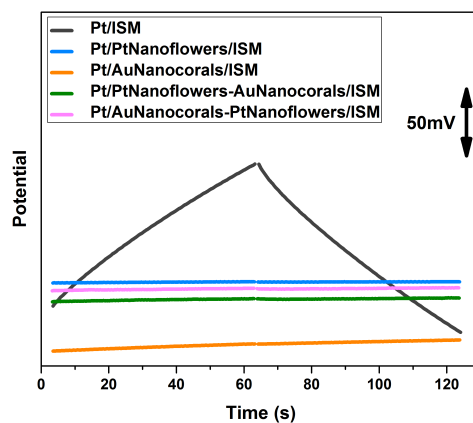
Figure 2.5: CRC measurements of AuNanocorals/PtNanoflowers (pink curve) and PtNanoflowers/AuNanocorals (green) SCs in comparison with the flat platinum electrode (black) and AuNanocorals (orange) and PtNanoflowers (blue) SCs. All curves were obtained with a Li^+ ISM in a 0.01M LiCl solution applying a current of ± 5 nA for 60s. [19]

2.3 Performance evaluation criteria of ISEs

The design and the development of a sensor strongly depends on the requirements of the final application. The most important parameters in a sensing system are:

- **Selectivity**: ability to measure the concentration of a substance in presence of other interfering substances.

- **Sensitivity**: ability to discriminate small variations of the analyte concentration.

- **Limit Of Detection (LOD)**: the minimum analyte concentration that can be reliably detected.

- **Dynamic Linearity Range**: ability to follow linearly variations of analyte concentration in a certain concentration window.

In addition, SC-ISEs must satisfy several properties in order to be used in portable devices: they must provide reproducible and precise results, possibly with calibration-free measurements; they must be biocompatible and show high stability over time in order to ensure the possibility of monitoring the patient for several hours (and eventually even longer) without calibration. Potential drift is known to be one of the most critical issues in ion sensing. In this regard, it is crucial to plan several tests to control the sensor performance. The most important sensor parameters will be described in more detailed below.

2.3.1 Sensitivity

It is fundamental to calibrate any sensor it in order to characterize its analytical performance. A calibration procedure results in the establishment of a calibration curve, that shows the relationship between the sensor output and the analyte concentration. In order to calibrate a sensor, its response (e.g. the open circuit potential for ISEs) is recorded at increasing and known concentrations of target analyte. The sensitivity is then defined as the slope of the calibration plot [14].

2.3.2 Limit of detection

The LOD is one of the most important parameters to characterize the sensor performance. In fact, it provides an indication of the smallest concentration of analyte that can be reliably measured. According to IUPAC definition, for the potentiometric ISEs the upper and lower LODs can be determined as the intercepts between different linear segments of the calibration curve [14].

2.3.3 Selectivity

One of the most crucial parameter of every sensor is its selectivity, i.e. the ability of a sensor to measure a concentration of a substance in presence of other interfering compounds. Sensor selectivity is never absolutely perfect, therefore, it is important to characterize it. IUPAC reports [20] used Nikolsky Eisenman equation, to compute the measured potential, with the presence of interfering ions:

$$E = E_0 + \frac{RT}{z_A F} In[a_A + \sum_B K_{A,B}^{pot} (a_B)^{\frac{z_A}{z_B}}] \tag{2.2}$$

- E_0: constant including the the standard potential of the electrode

- z_A and z_B: respective valence number of the target ion and the interfering ions.

- a_A and a_B: respective activity of the target ion and the interfering ion.

- $K_{A,B}^{pot}$: potentiometric selectivity coefficient of the target ion A against the interfering ion B.

If $K_{A,B}^{pot} < 1$ the sensor is more selective toward the target ion. Smaller is its value, higher is the selectivity. On the contrary, if $K_{A,B}^{pot} > 1$ the sensor is more selective toward the interfering ion, but this is an unusual situation. It is important to notice that Nikolsky Eisenman equation (2.2) is valid if only if :

1. Target and interfering ions show Nernstian response.

2. $K_{A,B}^{pot}$ must be constant.

3. Target and interfering ions must have the same charge(in case of the presence of mono and divalent ions, more complex equations will be used).

According to the IUPAC raccomandation two are the main methods for the determination of selectivity coefficient:

- Separate solution method (SSM) : uses two different solutions for the measurements. The first one contains only target ions A at activity a_A, the second one has only interfering ions B at activity $a_B = a_A$.

- Fixed InterferenceMethod (FIM) : uses solutions containing interfering ions at constant concentration and varying concentration of the target ions.

The procedures for both methods are further explained in the thesis.

2.4   State of the art in Solid-contact ISEs

Wearable all solid state ISEs represent approximately 25% of the total wearable electrochemical sensors described during the last decade in scientific journals [21]. Interestingly, this percentage indicates that SC-ISE technology is a trending topic in research. Hence, it is expected that SC-ISEs will enter in the industry of wearable devices soon. While this technology high potential, no commercial example exist in the market yet because some critical issues challenges still need to be overcome. The main limitations and current state-of-the-art of SC-ISEs technology are given below.

- **Potential instability** : The stability of the electrode is influenced by the potential drift and changes in environmental conditions (temperature, pressure, humidity). The potential drift can be caused by two factors: the formation of already mentioned water layer at the ISM/SC interface and the small but non-zero current required for OCP measurements[11, 15].

- **Recurrent calibration** : It is difficult to reach a very high reproducibility for the calibration slope of these sensors with consequent need of automation or qualified personnel. In this regard, the choise of the electrically conductive substrate can be crucial to achieve good reproducibility and short equilibration time.[11, 19].

- **Limit of detection** A low LOD is essential for a correct measurement of ion concentration. For this reason, proper ISM conditioning is imperative.

- **Biocompatibility** : In the case of on body sweat analysis, it is crucial to asses the toxicity effects from the materials used in the fabrication of the ISM especially because they are in direct contact with the individuals' skin [22].

A lot of example have been reported trying to overcome these limitations that show a clear preference for conducting polymers (CPs) or nanostructured materials. The main types of sensors for monitoring sweat ions are sweat bands, skin patches and garments. They differ from each other mainly in the way the sample reaches the electrodes. This can happen either through direct contact or through a recollection strategy. The description of some of theme is reported here.

Among the best characteristics of epidermal patches the most important is the high versatility for adaptability on the body, in fact different types of epidermal wearable devices, such as skin patches, tattoos and bandages, have been used to monitor the electrolytes in sweat, allowing the analysis of ion concentration in the regional parts of the body. Wang et al. presented two ISEs in a temporary-transfer tattoo platform for monitoring ammonium and pH levels in sweat [24, 23]. The electrodes structures for pH and $NH4^+$ sensing are given in 2.6. Regarding ammonium The
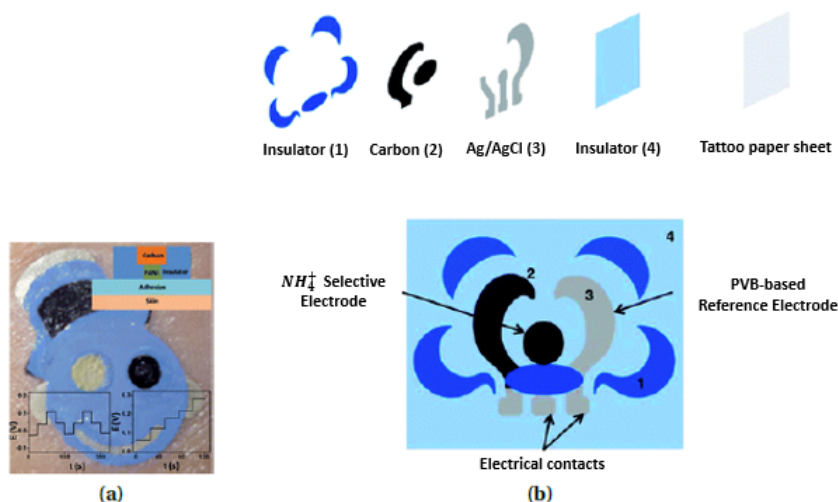
Figure 2.6: a) Picture of pH tattoed potentiometric sensor[23]. b) Structure of ammonium tattoed ISE [24].

resulting tattooed potentiometric sensor exhibits a working range between 10^{-4} M to 0.1 M well within the physiological levels of ammonium in sweat. For the pH exhibit rapid and sensitive response to a wide range of pH changes with no carry-over effects. The devices are resistent to mechanical deformations experienced by the human skin. However, the stability andentrainment characteristics of these sensors may be improved by implementing an ion-to-electron transducer between the membrane and conductive track.

In several works, paper substrates were used as substrate to reduce costs. The main advantage of using textiles is the possibility of adaptability of conventional manufacturing technologies to produce textile-based sensors compared with other wearable materials. A simple way to fabricate disposable potentiometric ion sensors is shown in [25]: a conductive paper is produced by dipping conventional filter paper in a suspension of carbon nanotubes in a water-surfactant mixture; this acts both as conductor and ion-to-electron transducer. They show good performance in comparisons with the classical K^+, NH4$^+$ and pH ISEs . Buhlmann et al. present a complete paper-based device for Cl^- and K^+ detection with integrated RE. The sensors have been tested both in aqueous and biological samples showing linear response and good reproducibility using a sample of only 20 µl. A polymeric ISE device with a SC made of poly(3-octylthiophene) (POT), a lipophilic conductive polymer, was fabricated on a carbon nanotube conductive paper[26].

Sweatbands are the most used platforms due to simple integration. The electrodes
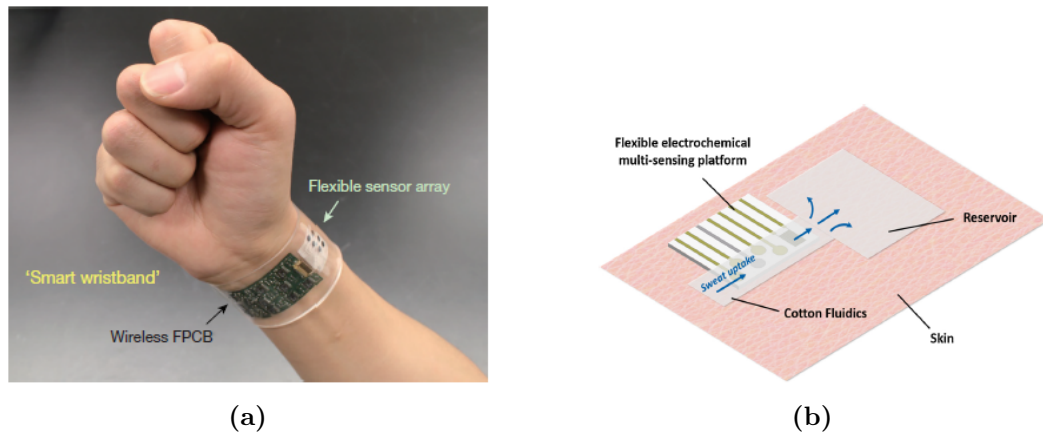
Figure 2.7: a) Fully integrated wearable band for perspiration analysis[27]. b) Scheme of the fluidics used in the complete wearable multi-electrodes system to ensure fresh sweat on the detection region and avoid direct contact of the sensors with the skin[28].

are usually prepared in a separate flexible substrate and then fixed on common bands. One of the most famous was reported in Nature in 2016 [27]. The wearable multi-sensing platform presented is a flexible and fully integrated sensors array which include K^+ and Na^+ ISEs for in situ perspiration analysis. The system is also coupled to an iontophoresis system to actively extract sweat from the eccrine glands. Another intersting example is given in [28] A wearable multi-electrode platform includes four electrodes for the simultaneous sensing of analytes, a temperature sensor and a stable reference electrode (RE) with an ionic-liquid junction. The interested ions are: Li^+ for Therapeutic Drug Monitoring (TDM) in psychiatric disorders, Pb^{2+} for the control of heavy metal contamination, K^+ and Na^+ for sport tracking.

Chapter 3

Procedures and techniques

In this paragraph, we will aboard all the processes we have executed to realize ISEs for the measurement of potassium, sodium, calcium and ammonium in sweat. First of all, we will present the methods and materials used for each step of the production. Afterward, we will display the opted measurement procedure for the calibration and selectivity. Hereby, the required steps for each ion sensing:

- Platinum nanostructuration

- Ion-Selective Membrane (ISM) deposition

- Conditioning

- Calibration

- Selectivity

3.1 Platinum nanostructuration

As already mentioned (paragraph 2.2.2), a nostructured materials use the electrical double layer formed at the membrane/electrode interface for ion-to-electron transduction. This leads to several advantages like avoiding the risk of water absorption, and the characterization of high capacitance values, property crucial to reduce polarization effects due to the small but non-zero currents required for the measurement. In literature, different combinations of nanostructures and substrates have been tested. Figure 3.1a and 3.1b respectively show the CRC(Current Reversal Chronopotentiometry) responses for platinum and gold substrate-based, by means of three different samples, for the reproducibility comparison. Platinum samples with nanoflowers SCs provide a pretty more stable response, compared to gold nanocorals.

(a) Pt substrate
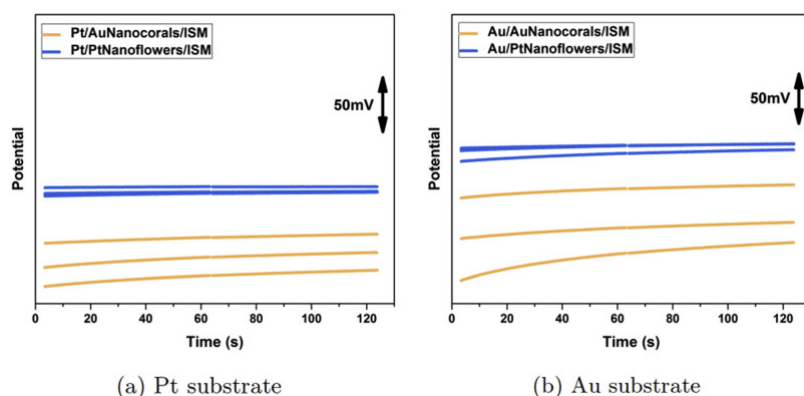
(b) Au substrate

Figure 3.1: Li+ potential reproducibility acquired across the ISM membrane, with the presence of nanostructured materials, with respect to the type of substrate.[19]

Considering the successful results of platinum nanopetals obtained by fast eletrode-position[19], compared to other nanostructured materials in other projects[15], we have decided to use the same nanostructures in our project, applying the same deposition procedure.

(a)

(b)
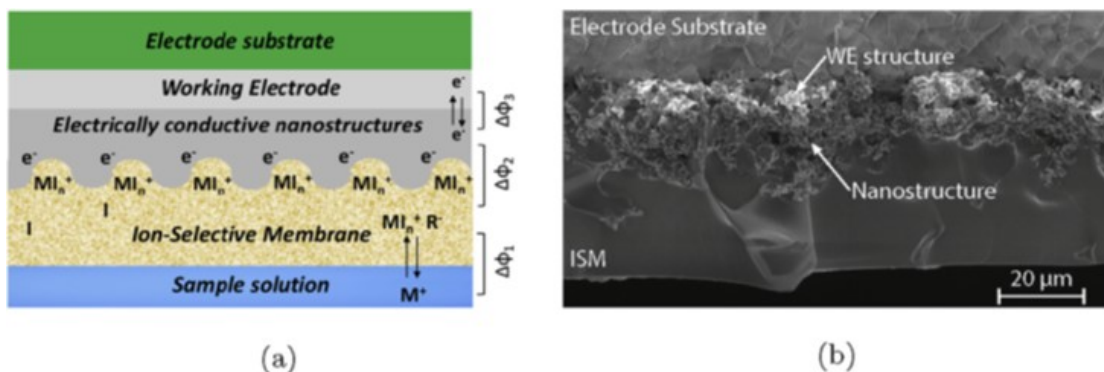
Figure 3.2: a) Scheme of the fabricated nanostructures-based SC-ISEs. b) SEM cross-sectional view of a ISE with platinum nanoflowers as SC. Reprinted from [19].

Platinum Screen Printed Electrodes (SPEs) with an active area of 12.56 mm^2 were purchased from Metrohm (Switzerland). Chronoamperometry (CA) was used to obtain the nanopetals deposition on the surface of the platinum(Pt) substrate, using a solution containing a divalent platinum salt (25m[M] K2PtCl4 and 50m[M] H2SO4). 10ml of the platinum salt solution was poured into a beaker where a stirrer was placed. Two Screen-Printed Electrodes(SPEs) were dipped in the solution, by means of cables connectors for SPEs. A Voltage of 1V for more than 100[s] was applied. We had to be aware that, the electrodes are well dipped in

the solution and they are parallel in front of each other, setting the stirring at 120 rpm. CA measurements were carried out, using the Autolab potentiostat under a computerized control (Metrohm, Switzerland). After deposition, the electrode was taken out and washed in water and dried with compressed air. An example of the utilized setup is shown in Figure 3.3.
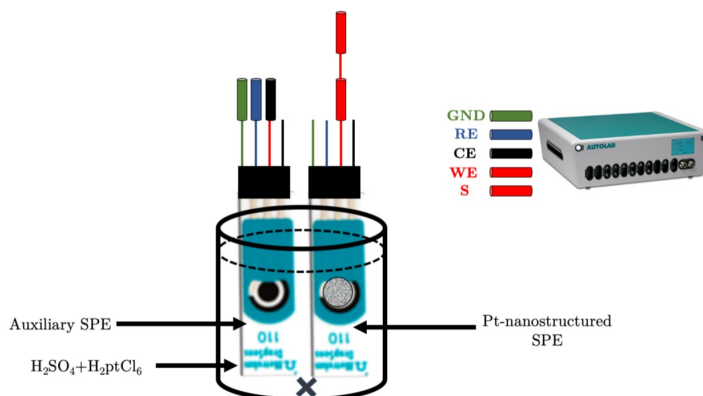
Figure 3.3: Platinum nanostructuration setup.

3.2   Ion Selective membrane

For the realization of ISMs we will test the ionophores and corresponding cocktails recommended available, proposed by Sigma(Switzerland). All chemicals have been purchased from Merck (Germany), unless otherwise stated. These include: H2SO4, KCl, NaCl, $CaCl_2$, NH_4CL, LiCl, $MgCl_2$, valinomycin (K ionophore I), 4-tert-butylcalix[4]arene-tetraacetic acid tetraethyl ester (Na ionophore X), Nonactin (NH_4 ionophore I), N,N-Dicyclohexyl-N,N-dioctadecyl-diglycolic diamide (Calcium ionoohre IV), 2-nitrophenyl octyl ether(o-NPOE), potassium tetrakis(4-chlorophenyl)borate, bis(2-ethylhexyl) sebacate (DOS), polyvinyl chloride (PVC), THF, acetic acid, uric acid, DL-lactic acid, ascorbic acid, glucose, pyruvic acid glutamic acid, urea. Ionophores, also called ion carrie, are molecules consisting in facilitating ion passage in or out of cell membrane. It is a substance capable to transfer ions from a hydrophilic medium, such as water, into a hydrophobic medium, such as a biological membrane. The mechanism is based on binding to particular ions driving them through the hydrophobic environment of a cell membrane, forming for example ions channels. Another essential element in the membrane cocktail is the plasticizer. Different types of plasticizers are often used to prepare the membrane electrodes. They have the ability to interact with polymer chains, providing flexibility, durability, and mobility [11]. On top of the plasticizing

effect, they are able to modulate drug release profiles. The selection of a plasticizer is an important part, since it can affect strongly both LOD and selectivity. Small amounts of lipophilic ions are added in the cocktail in order to ensure Nernstian behaviour [11] and avoid extracting a consequent amount of counterions from the sample solution to the Ion-Selective Membrane. Indeed, the membrane should be exclusively permeable to ions of the same sign of the target ion. Another important compound in the cocktail is the Poly(vinyl chloride)(PVC) [29] that consists in increasing the dielectric constant so that comparatively high ionic concentrations are present. The PVC has also the role of holding together the membrane. The cocktail is prepared in tetrahydrofuran (THF), in order to make the mixture homogeneous.

Sodium-selective membrane		
Ionophore	Sodium Ionophore X	0.7mg
Lipophilic anionic site	Potassium tetrakis(4-chlorophenyl)borate	0.2mg
Plasticizer	2-Nitrophenyloctylether (o-NPOE)	64mL
Polymerizer	Poly(vinyl chloride) (PVC)	33mg

Table 3.1: Sodium-selective membrane composition.

Potassium-selective membrane		
Ionophore	Potassium Ionophore I	1mg
Lipophilic anionic site	Potassium tetrakis(4-chlorophenyl)borate	0.5mg
Plasticizer	bis(2-ethylhexyl)sebacate (DOS)	72mL
Polymerizer	Poly(vinyl chloride) (PVC)	33mg

Table 3.2: Potassium-selective membrane composition.

Calcium-selective membrane		
Ionophore	Calcium Ionophore IV	1mg
Lipophilic anionic site	Potassium tetrakis(4-chlorophenyl)borate	0.28mg
Plasticizer	2-Nitrophenyloctylether (o-NPOE)	63.3mL
Polymerizer	Poly(vinyl chloride) (PVC)	32.9mg

Table 3.3: Calcium-selective membrane composition.

Ammonium-selective membrane		
Ionophore	Ammonium Ionophore I	1mg
Plasticizer	bis(2-ethylhexyl)sebacate (DOS)	73.1mL
Polymerizer	Poly(vinyl chloride) (PVC)	32.2mg

Table 3.4: Ammonium-selective membrane composition.

For each membrane preparation, a 5 ml beaker and 1 straight stirrer are used. A pipette with the liquid chemical and 1 ml syringe with a long needle with the THF was prepared. The further step of the preparation consisted in adding all the remaining liquid chemicals and stirring for a couple of minutes. $10\mu l$ of the obtained mixture was drop-casted on the electrodes, followed by drying at dark for 24h for the solvent evaporation

3.3 Conditioning

Proper membrane conditioning is needed in order to make the membrane enough stable and sensitive in a specific concentration range [14, 30]. Before performing any ISE measurements, conditioning is required. The membrane needs to be exposed to the target ion for several hours, before the calibration. Since the sensing performance depends on the conditioning concentration and conditioning time, we have performed a calibration for each ion at low conditioning of 1m[M] and high conditioning of 10m[M].

3.4 Calibrartion in water

Calibration were carried out by potentiometry, consisting in performing the OCP measurements, by means of an Autolab potentiostat with Nova Software (Metrohm, Switzerland). All potentiometric measurements were achieved, with a Ag/AgCl double junction reference by Metrohm. Indeed, potentiometric measurements consist in measuring the potential, so-called, open circuit potential measurement, of the solution between the reference electrode and the working electrode (WE), with a quasi-zero current (1n[A]) across the system. In other words, an OCP measurement consists in measuring the equilibrium condition between the working electrode and the electrolyte in an interval time T (T=50[s] in our project), after introduction of a target ion concentration.
The calibration technique was performed by injecting different concentration values of the target ion in the electrolyte (water) at each constant interval time.In order to do the calibration curve (Figure 3.4) the steady potentials was extracted at
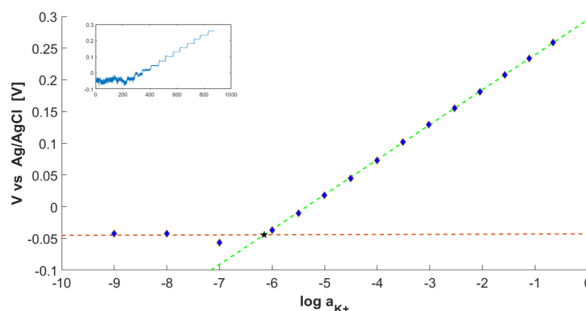
Figure 3.4: Example of calibration curve.

each calibration step plotted them against the activity of the target ion at the corresponding step.

3.5 Selectivity coefficient

The intensity of the interference, produced by different ions on a target ion, is expressed by the selectivity coefficient. The selectivity coefficients are determined, using two different well-known methods, such as: the Fixed Interference Method (FIM) and the Separated Solution Method (SSM).

3.5.1 Separate solution method (SSM)

Separated solution method consists in calibrating the interfering ions and comparing the responses by the target membrane. The calibrations were performed in function of different interfering ions in order of their adsorption capacity. The following table present the ascending order of calibrations, according to the target ion: The

ISE	Interfering Ions
Sodium-selective electrode	Mg2+ | Ca2+ | NH4+ | Li+ | K+
Potassium-selective electrode	Mg2+ | Ca2+ | Li+ | Na+ | NH4+
Ammonium-selective electrode	Mg2+ | Ca2+ | Li+ | Na+ | K+
Calcium-selective electrode	K+ | Na+ | Li+ | Mg2+

Table 3.5: Interfering ion for each ISE.

calibration procedure is the following:

1. Condition the ISEs in the lowest interfering ion, at 3mM, for 48h.

2. Perform ISE calibration for the J interfering ion in order of increasing interference. Rinse the SPE quickly in pure water between each calibration.

22

3. If the calibration curve with an interfering ion J is Nernstian, extract the potential E_J at an activity a_J that falls in the Nernstian portion of the curve.

4. Perform ISE calibration with the target ion I.

5. If the calibration curve with the target ion I is Nernstian, extract the potential E_I at an activity a_I that falls in the Nernstian portion of the curve. Extract the sensitivity s.

6. Compute the selectivity coefficient as:

$$logK_{I,J}^{pot} = \frac{z_I}{s}(E_J - E_I) + log(\frac{a_I}{a_J^{\frac{z_I}{z_J}}}) \tag{3.1}$$

7. Iterate the procedure for all interfering ions.

3.5.2 Fixed interference method (FIM)

Fixed Interference Method consists in performing calibrations of the target ion, with different interfering backgrounds. The calibration procedure is the following:

1. Condition the ISEs in the target ion, at 3mM, for 24h.

2. Perform ISE calibration with the primary ion I only.

3. Perform ISE calibration with the primary ion I, in presence of an interfering ion J at a concentration c_J=3.3mM if z_J=1 or $c_J = 4.5$mM, if $z_J = 2$.

For the calibration curve in presence of an interfering ion J, extract the lower LOD, a_I(LDL) and compute the selectivity coefficient as:

$$logK_{I,J}^{pot} = log(\frac{a_I(LDL)}{a_J^{\frac{z_I}{z_J}}}) \tag{3.2}$$

23

3.6   Sensor characterization in artificial sweat

Artificial sweat was prepared according to the composition reported in Table 3.6 [31]. In order to do the calibration in artificial sweat condition the sensors 24h before the calibration, in the target analyte, at 1 or 10mM. Then, perform sensor calibration in water background and in artificial sweat background electrolyte.

Compound	Concentration
NaCl	0.34M
NH4Cl	0.33M
Acetic acid	0.08M
DL-Lactic acid	0.20M
Ascorbic acid	10 μM
Glucose	0.17mM
Uric acid	59μM
Pyruvic acid	0.18mM
Glutamic acid	0.37mM
Urea	10mM

Table 3.6: Composition of artificial sweat.

Chapter 4

Results

4.1 Conditioning and calibration in water

For each of the four ions chosen in this work i.e. sodium potassium calcium and ammonium have been prepared 5 SC-ISEs samples. For all the calibration two different conditioning were tested corresponding to 1[mM] and 10[mM]. The best sample for each ion will be presented.
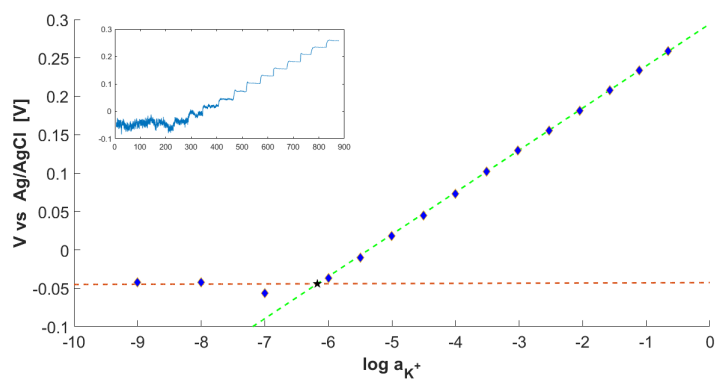

**Figure 4.1:** Potassium SC-ISE calibration curve in water background
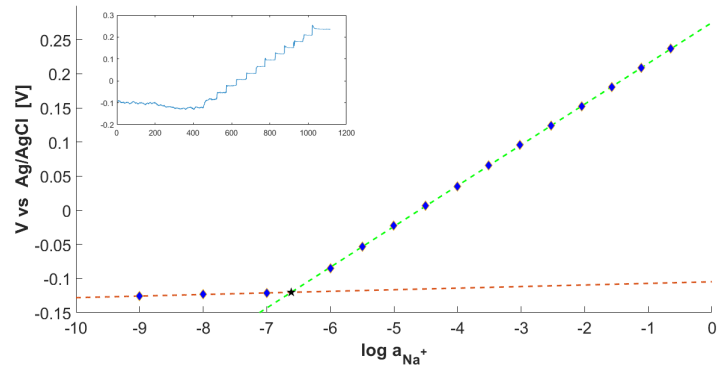
**Figure 4.2:** Sodium SC-ISE calibration curve in water background
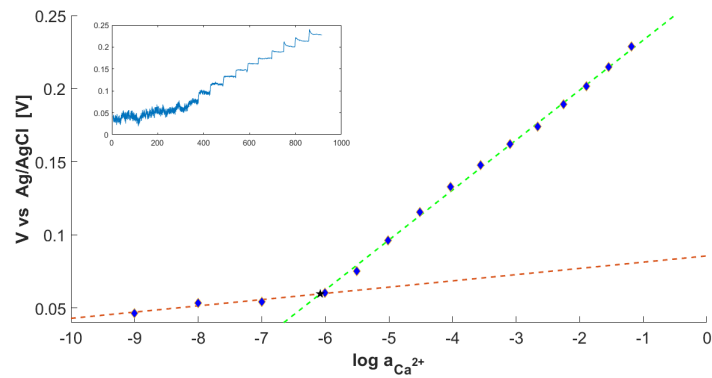
Figure 4.3: Calcium SC-ISE calibration curve in water background
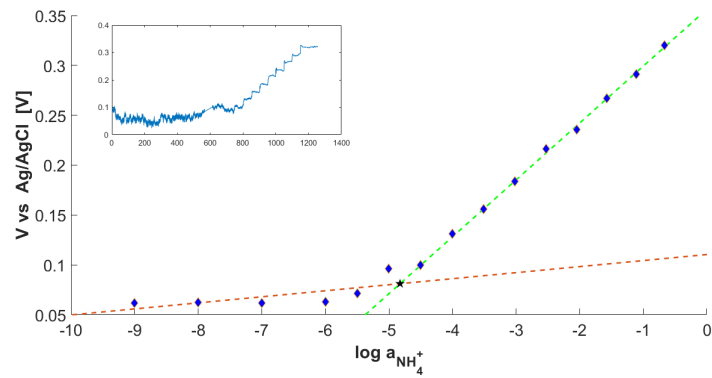

Figure 4.4: Ammonium SC-ISE calibration curve in water background

As discussed in the previous section, the conditioning procedure is crucial to ensure

proper functioning in the range of interest. For this reason, two conditioning concentrations were tested and compared for all ions. All ISEs show near-Nernstian slope and a very good limit of detection for all four the analyte investigated. Regarding ammonium and calcium ISEs no significant effect of the conditioning procedure on the sensitivity values and its standard deviation is found, on the contrary the LOD is about half a decade smaller with reduced standard deviation values when a low concentration solution is used. On the contrary to what could be expected for potassium and sodium sensors, the solution with the higher concentration leads to more stable results in terms of sensitivity and LOD.

	Sensitivity (mV/dec)	LOD (µM)	Concentration in Sweat (mM)
Potassium	$50,945 \pm 2,90$	$1,15 \pm 0,35$	1-24
Sodium	$56,246 \pm 1,093$	$0,302 \pm 0,072$	10-100
Calcium	$25,883 \pm 1,07$	$0,64 \pm 0,25$	0,41-12,4
Ammonium	$52,808 \pm 3,377$	$14,709 \pm 11,312$	0,1-8

Table 4.1: ISEs calibration in water background

Table 4.1 shows the sensitivity and LOD for each sensor obtained compared with the concentration range of the corresponding analyte in the sweat under rest conditions.

4.2 Interference

FIM and SSM were performed. All the samples have been prepared and tested for each method. The obtained values were compered with those found from literature.

	Mg^{2+}	Ca^{2+}	Li^+	Na^+	$NH4^+$
This work by FIM	$-6,57 \pm 0,82$	$-5,57 \pm 0,27$	$-2,02 \pm 0,11$	$-1,796 \pm 0,09$	$-1,05 \pm 0,31$
Literature by FIM [25]	-3,9	-4,6	-3,6	-4,6	-2,1
This work by SSM	$-2,5 \pm 0,58$	$-1,74 \pm 0,48$	$0,119 \pm 0,42$	$-0,23 \pm 0,44$	$0,53 \pm 0,04$
Literature by SSM [32]	-6,7	-7,8	-4,6	-4,7	-2,0

Table 4.2: Potassium ISEs interference studies by FIM and SSM

	Mg^{2+}	Ca^{2+}	NH4$^+$	Li$^+$	K$^+$
This work by FIM	-10,12 $\pm$ 0,79	-7,41 $\pm$ 2,70	-5,97 $\pm$ 0,93	-5,16 $\pm$ 0,36	-5,20 $\pm$ 0,35
Literature by FIM [33]	-3.8	-3.5	n.a.	-3.1	-1.8
This work by SSM	-2,40 $\pm$ 0,66	-3,99 $\pm$ 1,22	-5,05 $\pm$ 0,75	-3,24 $\pm$ 0,14	-3,94 $\pm$ 0,33
Literature by SSM [34]	-3.3	-3.2	-4,9	-3.0	-4.8

Table 4.3: Sodium ISEs interference studies by FIM and SSM

	K$^+$	NA$^+$	Li$^+$	Mg^{2+}
This work by FIM	-6,53 $\pm$ 1,67	-6,31 $\pm$ 0,81	-6,49 $\pm$ 0,66	-6,82 $\pm$ 1,77
Literature by FIM [35]	-3,1	-4,0	n.a.	-3,8
This work by SSM	-9,42 $\pm$ 1,34	-8,75 $\pm$ 2,08	-10,4 $\pm$ 1,45	-6,79 $\pm$ 2,37
Literature by SSM [36]	-7,5	-5,9	-5,8	-4,4

Table 4.4: Calcium ISEs interference studies by FIM and SSM

	Mg^{2+}	Ca^{2+}	Li$^+$	NA$^+$	K$^+$
This work by FIM	-7,58 $\pm$ 0,70	-7,28 $\pm$ 1,40	-3,40 $\pm$ 1,62	-3,00 $\pm$ 1,85	-1,00 $\pm$ 0,84
Literature by FIM [37]	n.a.	-4,2	-3,6	-2,9	-0,8
This work by SSM	-3,10 $\pm$ 2,04	-2,90 $\pm$ 1,55	-2,24 $\pm$ 1,45	-2,15 $\pm$ 1,37	-1,04 $\pm$ 0,44
Literature by SSM [38]	-5,5	-4,8	-3,6	-2,9	-0,8

Table 4.5: Ammonium ISEs interference studies by FIM and SSM

The values obtained by the SSM and the FIM are reported in Table 4.2, Table 4.3, Table 4.4 and Table 4.5 with the comparison with the highest values reported in literature for conventional all-solid-state ISEs. High selectivity is achieved for all realized SC-ISEs against all most common ions. With the exception of a few values, in general both SSM and FIM coefficients are comparable with the lowest literature values. As expected, the highest interference is due to Na$^+$ and K$^+$ for K$^+$ and Na$^+$ ISEs, respectively. This is due to the similar sizes of the ions. Regarding Ca ISEs, is to be noted that for both FIM and SSM the value of selectivity coefficient obtained in this work are all quite better than that found in literature. Also the Ammonium membrane, in the presence of interfering ions showed a good response, as expected the most interfering ion is K$^+$.

4.3   Testing in artificial sweat

Figures 4.5, 4.6,4.7 and 4.8 shows the calibration curve of a K^+ Na^+ Ca^{2+} and NH_4^+ SC-ISE and in sweat after a one day conditioning in 10 mM KCl NaCL and 1 mM $CaCl_2$ NH4CL, respectively.
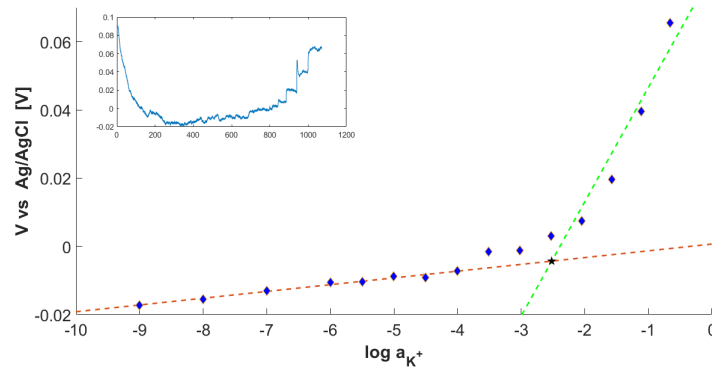
Figure 4.5: Potassium SC-ISE calibration curve in artificial perspiration background.
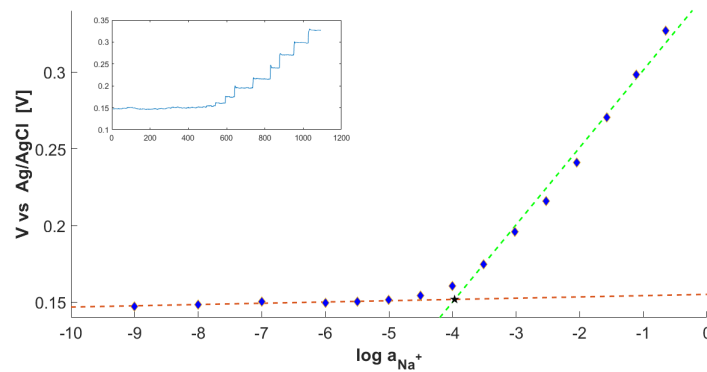
Figure 4.6: Sodium SC-ISE calibration curve in artificial perspiration background
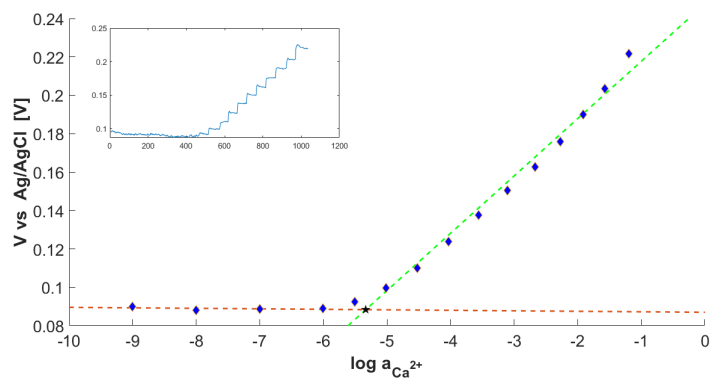
Figure 4.7: Calcium SC-ISE calibration curve in artificial perspiration background.
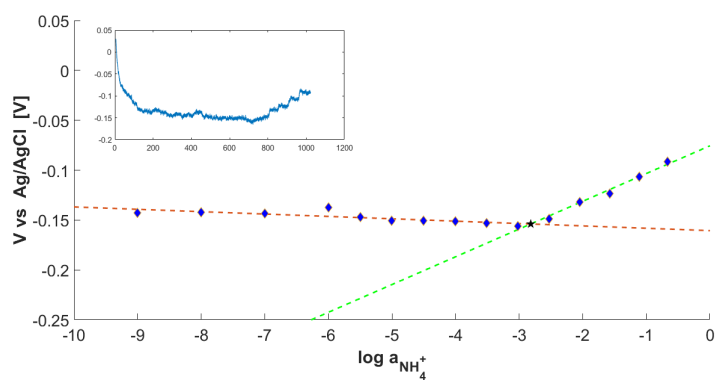
Figure 4.8: Ammonium SC-ISE calibration curve in artificial perspiration background.

The corresponding time trace from the calibration curves were obtained are reported in the small inset on the top left corner of each graph. Sharp steps and stable responses over time are achieved in both cases after analyte addition. A summary of the analytical parameters obtained from the calibration curves of five different samples is given in Tables 4.6.

	Sensitivity (mV/dec) Water	Sensitivity (mV/dec) Artificial Sweat	LOD (µM) Water	LOD (µM) Artificial Sweat
Potassium	50,94 ± 2,90	42,98 ± 5,48	1,15 ± 0,35	2412 ± 361
Sodium	56,24 ± 1,093	47,07± 6,44	0,302 ± 0,072	60,42 ± 30
Calcium	25,88 ± 1,07	28,79± 3,40	0,64 ± 0,25	5,31 ± 1,43
Ammonium	52,81 ± 3,377	38,32 ± 6,51	14,70 ± 11,31	4057 ± 1723

Table 4.6: Analytical parameters in artificial sweat.

In all cases, quasi-Nernstian slopes are attained by the sensors. The presence of more interactions in artificial sweat with respect to aqueous solutions results in a slightly higher standard deviation for the sensitivity. On the contrary, the LOD is highly affected by the presence of other compounds in solution. In particular, a reduction of about three orders of magnitude for K^+, two order of magnitude for NA^+ and NH_4^+ and one order of magnitude for Ca^2+ is observed when measuring,in artificial sweat with respect to aqueous solution. The LODs in water solution are similar to the ones reported in literature. No values in artificial sweat have been found in literature for comparison. The obtained values are indeed below the physiological concentration ranges(up to 18.5mM for K^+, 90mM for NA^+, 90.4mM for NH_4^+, 12.4 mM for Ca^2+ during physical exercise). Some improvements might be useful to futher improve the measurement accuracy, especially for K^+ and NH_4^+ sensors. In this regard, the conditioning procedure might be properly tuned to lower further the LOD.

Chapter 5

Muscle fatigue and exercise protocol

Muscle fatigue is a very frequent condition in the every day life of each of us, iIn fact, it involves from the athlete to the patient in rehabilitation for the recovery of limb functions. For this reason, a wide variety of exercise models, protocols and assessment methods have been studied, but the processes that cause it and an easy way to identify it are far from being identified. Muscle fatigue is a complex phenomenon depending from various causes and mechanisms. It occurs after the result of a chain of metabolic, structural and energy changes in the muscles caused by an insufficient supply of oxygen and nutrients through the blood circulation and due to changes in the efficiency of the nervous system. Referring to [39] the potential sites of neuromusclar fatigue can be divided in central fatigue, fatigue of the neuromuscular junction and local muscle fatigue. In recent decades, research has sought to describe how fatigue is generated in different exercises and the mechanisms involved in the processes, but there are different views of the processes associated with fatigue. We describe in this chapter the most common method for assessing muscle fatigue, which organic compounds are involved and an alternative method based on the concentration of ions in sweat.

5.1 EMG Signal

The most used method to measure muscle fatigue is the study of the surface EMG signal(sEMG). In fact, the myoelectric signals recorded reflect the biochemical and physiological changes in muscles during fatiguing contractions. The surface electrodes detect the electrical activity of the surface muscles and the amplitude and power spectrum of the signal can be determined. The amplitude reflects the number and size of action potentials in the muscle over a given period [40, 41].

The most common used criteria are the root mean square (RMS) and conduction velocity (CV) regarding the temporal domain of the signal and the mean and median frequency (MF) evaluated from the spectrum of the signal. Although fatigue is most often the consequence of practicing movement and exercise (sports training, limbs rehabilitation, ergonomics), the majority of studies in the past were focused to quantify muscle fatigue resulting from isometric (constant length muscle contractions). Principally because during dynamic contractions, several factors, such as the change in the number of active motor units and the change in muscle fiber conduction, lead to a major non-stationarity of the myoelectrical signal [42, 43]. Therefore, it's more difficult to compute the parameters commonly used as indicators of spectral changes (i.e. median and mean frequency) during dynamic contractions and they may not accurately reflect muscle fatigue. In the last decade, recent development in time-frequency analysis suggested that Choi-Williams distribution and continuous wavelet transform are the most suitable method to be applied to non-stationary sEMG signal compered to the classic short time fourier transform. Despite the presented limitations and the possible problems of cross talk of myoelectric signals from neighbouring muscles [44] the sEMG measurement is most used method to evaluate local muscle fatigue. Its principal advantages, hence, are non-invasiveness, applicability in situ, real-time monitoring.

5.2 Muscle strain biomarkers

The concentration of lactate, ammonia and other compounds based on a blood sample are indicative of the muscle fatigue in a muscle. This is possible because, after the contraction of a muscle, besides the type and size of the muscle fibres, blood flow is increased due to the pumping effect. At a certain level of contraction, blood flow is stopped by intramuscular pressure and the muscle becomes ischemic. The increased concentrations of the biomarkers is responsible for fatigue by change the intracellular pH. This behavior is also responsible for the variation in the myoelectric signals. It leads to a reduction of muscle fibre conduction velocity (CV) and as consequences the decrease of median frequency (MF) and the increase in sEMG signal amplitude [45]. Due to the way to collect blood sample, and how it is analyzed in order to obtain the interested compounds concentrations, it is not feasable to monitor the state of fatigue in real-time. In order to solve those issues, exploiting the correlation between blood and sweat, we propose the use of the SC-ISEs realized in this work. Indeed, as already written in 1.3 the concentration of potassium, sodium, calcium ammonium can provide not only an indication of muscle fatigue but also the state of hydration and bone mineral loss in a non-invasively and continuous way.

33

5.3   Cycling experimental protocol

In orders to assess the goodness of our sensors in the estimation of muscle fatigue we developed a protocol for measure the sEMG signal of lower limb and the concentration of ions in sweat at the same time. The exercise that easily allows both the production of sweat and the fatigue of the hind limbs is the indoor exercise bike. The activity consists in a graded load exercise which involved a 5-min rest, 20-min cycling at 60 rpm after the starts of perspiration followed by cycling at 90 rpm until volitional fatigue, and a 10-min recovery period (Figure 5.1).
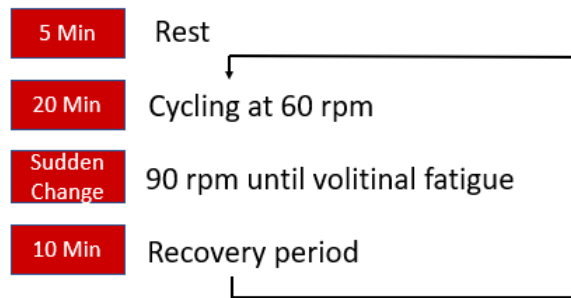
Figure 5.1: Cycling experimental protocol scheme.

As demonstrated in other works [27], the dramatic increase in the exercise power output from 60 rpm to 90 rpm immediately leads to abrupt elevations of heart rate, minute ventilation and V_O2 inducing muscle fatigue and therefore a variation of concentration of ions in sweat. Meanwhile the surface EMG signals of the rectus femoris, vastus lateralis, vastus medialis and gastrocnemius are acquired as it has been suggested to be the principal power producers during cycling exercise (Figure5.2).
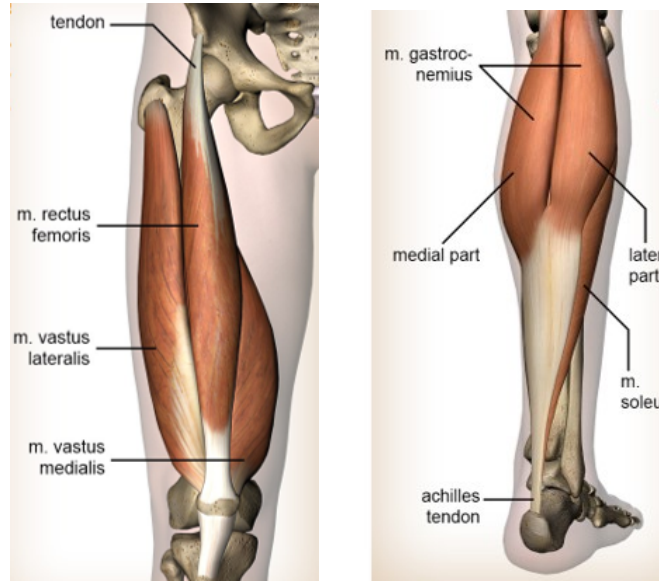
Figure 5.2: Muscle involved during cycling exercise.

5.4   Data Analysis

The EMG were recorded with a Noraxon Desktop DTS wireless system at a sampling rate of 1.5 kHz by using superficial Ag-AgCl electrodes (Kendall H124SG, ECG electrodes 30 × 24 mm) after appropriate skin preparation. Electrodes were placed according to guidelines of the Surface Electromyography for the Non-Invasive Assessment of Muscles European Community project (SENIAM) [46]. EMG data were preprocessed offline using MATLAB (MathWorks, Natick MA). The raw EMG signals were detrended, band-pass filtered 50–500 Hz (Butterworth filter, 7th order). Then, the cycles were extracted from the signals according to temporal criteria and amplitude thresholds. From each cycle root mean square (RMS) and Median frequency (MF) (i.e. frequency which 'cuts' the spectrum of the signal into two parts having an equivalent area) were evaluated as two of the most used criteria suggested and compared in muscle fatigue assessment [45, 47, 48]. RMS(5.1) MF(5.2) are defined as follow:

$$RMS = \sqrt{\frac{\sum_n^{i=1} |rawData_i|}{n}} \qquad (5.1)$$

- i : order number of the dealing sample point

- rawData: value of the ith sample point

- n: total number of the data points

$$\int_0^{MF} S(f)df = \int_{MF}^{f_n} S(f)df = \frac{1}{2}\int_0^{f_n} S(f)df \qquad (5.2)$$

- f: frequency

- S(f) : power at frequency f

- f_N : Nyquist frequency

Figure 5.3 shows an example of the RMS and MF traces[1] of the vastus lateralis EMG. As can be seen throughout the exercise with graduated load there is a gradual rise in the RMS and a gradual decline in the MF. In the moment of sudden change of RPM of the bicycle, as expected, there is an important increase in the RMS and a significant decrease in the MF and then tends to return to initial conditions during the cool-down.
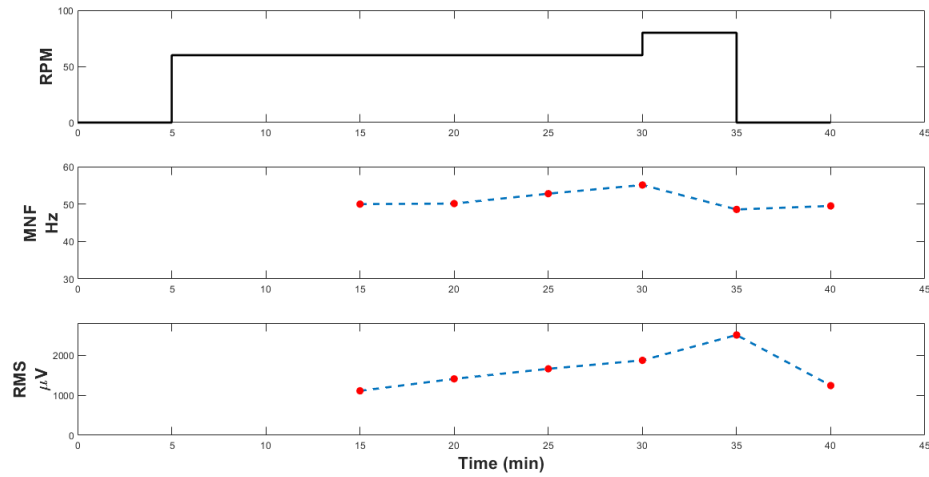

Figure 5.3: RMS and MF trace of Vastus lateralis EMG during the experimental cycling protocol.

---

[1]The RMS and MF traces begin at minute 15 because it is from that moment that the subject's sweating began.

36

Chapter 6

Conclusion and future work

Sweat has been deeply investigated in recent years, for Therapeutic Drug Monitoring [19] or for controlling the balance of electrolytes in human body [27, 28], to avoid frequent blood analysis, and improve the quality life of the patients. Indeed, sweat contains several ions that may substitute blood, avoiding an invasive method of ions uptake. This work investigates and addresses some of the challenges related to sweat sensing, with particular interest on the field of muscle fatigue. Unfortunately, due to timing problems in obtaining the approval of the scientific ethics committee, it was not possible to proceed with the measurements on humans with the ion sensors we made. We remain however many optimists thanks to the results obtained in the quality of the project and we believe that in the near future it will be possible to carry out a campaign of measures using the protocol we have devised. The main contributions of this thesis are summarized below:

- The fabrication of highly stable Potassium, Sodium, Calcium and Ammonium all-solid-state SC-ISEs exploiting platinum nanostructures by fast electrode-position procedures.

- For the first time, the possibility of measuring the concentration of ions in sweat and the EMG signal was considered in order to quantify muscle fatigue. A new cycling experimental protocol has been development in order to do these two different measurements at the same time.

- All the documents to submit a request to the ethical committee of the canton Vaud for a research campaign in order to test the sensors made on the human body in real perspiration have been prepared.

The results proposed in this project confirm the great development in recent years in this field. However, further research needs to be carried out to improve the system. Some interesting aspects for future work are reported here:

- Realization of lactate biosensor. As explained previously, lactate is a sweat biomarker extremely related to the muscle fatigue, so its realization can be a great improvement for the measure of muscle fatigue. In this work we tried to realize this sensor. Unfortunately, probably due to the modality of attachment of the enzyme or the quality of the enzyme itself we have not been able to obtain satisfactory results.

- Discordant opinions have been found in the literature on the effective efficacy of EMG parameters for assessing muscle fatigue especially for non-isokinetic contraction. We feel confident that in realms of biomechanical research the presented methods will be further developed, exercised, improved and standardized by adding ion sensing too.

- The design and realization of a complete flexible electrochemical multi-sensing system for ion monitoring in sweat

We hope that the present work will open up new perspectives and boost further research in the promising field of sweat sensing related to the muscle fatigue.

Bibliography

[1] Giusy Matzeu, Claudio Zuliani, and Dermot Diamond. «Solid-Contact Ion-Selective Electrodes (ISEs) based on Ligand Functionalised Gold Nanoparticles». In: *Electrochimica Acta* 159 (Mar. 2015), pp. 158–165. DOI: `10.1016/j.electacta.2015.01.143` (cit. on pp. 1, 3).

[2] Antonio Mena-Bravo and María Castro. «Sweat: A sample with limited present applications and promising future in metabolomics». In: *Journal of pharmaceutical and biomedical analysis* 90C (Dec. 2013), pp. 139–147. DOI: `10.1016/j.jpba.2013.10.048` (cit. on p. 1).

[3] Christopher Legner, Upender Kalwa, Vishal Patel, Austin Chesmore, and Santosh Pandey. «Sweat sensing in the smart wearables era: Towards integrative, multifunctional and body-compliant perspiration analysis». In: *Sensors and Actuators A: Physical* 296 (July 2019). DOI: `10.1016/j.sna.2019.07.020` (cit. on pp. 1–3).

[4] Giusy Matzeu, Larisa Florea, and Dermot Diamond. «Advances in wearable chemical sensor design for monitoring biological fluids». In: *Sensors and Actuators B: Chemical* 211 (May 2015), pp. 403–418. DOI: `10.1016/j.snb.2015.01.077` (cit. on p. 3).

[5] Amay J. Bandodkar, Itthipon Jeerapan, and Joseph Wang. «Wearable Chemical Sensors: Present Challenges and Future Prospects». In: *ACS Sensors* 1.5 (2016), pp. 464–482. DOI: `10.1021/acssensors.6b00250`. eprint: `https://doi.org/10.1021/acssensors.6b00250`. URL: `https://doi.org/10.1021/acssensors.6b00250` (cit. on p. 3).

[6] Robert Robergs, Farzenah Ghiasvand, and Daryl Parker. «Biochemistry of exercise-induced metabolic acidosis». In: *American journal of physiology. Regulatory, integrative and comparative physiology* 287 (Oct. 2004), R502–16. DOI: `10.1152/ajpregu.00114.2004` (cit. on p. 3).

[7] Susan M. Shirreffs and Michael N. Sawka. «Fluid and electrolyte needs for training, competition, and recovery». In: *Journal of Sports Sciences* 29.sup1 (2011). PMID: 22150427, S39–S46. DOI: `10.1080/02640414.2011.614269`.

eprint: `https://doi.org/10.1080/02640414.2011.614269`. URL: `https://doi.org/10.1080/02640414.2011.614269` (cit. on p. 3).

[8] Michael Chung, Giuseppino Fortunato, and Norbert Radacsi. «Wearable flexible sweat sensors for healthcare monitoring: a review». In: *Journal of The Royal Society Interface* 16.159 (2019), p. 20190217. DOI: `10.1098/rsif.2019.0217`. eprint: `https://royalsocietypublishing.org/doi/pdf/10.1098/rsif.2019.0217`. URL: `https://royalsocietypublishing.org/doi/abs/10.1098/rsif.2019.0217` (cit. on p. 3).

[9] Lindsay Baker. «Sweating Rate and Sweat Sodium Concentration in Athletes: A Review of Methodology and Intra/Interindividual Variability». In: *Sports Medicine* 47 (Mar. 2017), pp. 1–18. DOI: `10.1007/s40279-017-0691-5` (cit. on p. 4).

[10] Marc Parrilla, María Cuartero, and Gaston Crespo. «Wearable Potentiometric Ion Sensors». In: *TrAC Trends in Analytical Chemistry* 110 (Nov. 2018). DOI: `10.1016/j.trac.2018.11.024` (cit. on p. 4).

[11] Jinbo Hu, Andreas Stein, and Philippe Buhlmann. «Rational design of all-solid-state ion-selective electrodes and reference electrodes». In: *TrAC Trends in Analytical Chemistry* 76 (Dec. 2015), pp. 102–114. DOI: `10.1016/j.trac.2015.11.004` (cit. on pp. 6–10, 14, 19, 20).

[12] Eric Bakker, Philippe Buhlmann, and E. PRETSCH. «ChemInform Abstract: Carrier-Based IonSelective Electrodes and Bulk Optodes. Part 1. General Characteristics». In: *Cheminform* 29 (Mar. 2010). DOI: `10.1002/chin.199811318` (cit. on p. 7).

[13] Philippe Buhlmann and Li Chen. «Ion-Selective Electrodes With Ionophore-Doped Sensing Membranes». In: vol. 5. Mar. 2012. ISBN: 9780470746400. DOI: `10.1002/9780470661345.smc097` (cit. on p. 7).

[14] Erno Lindner and Róbert Gyurcsányi. «Quality control criteria for solid-contact, solvent polymeric membrane ion-selective electrodes». In: *Journal of Solid State Electrochemistry* 13 (Jan. 2008), pp. 51–68. DOI: `10.1007/s10008-008-0608-1` (cit. on pp. 7, 8, 12, 21).

[15] Irene Taurino, Gabriella Sanzó, Franco Mazzei, Gabriele Favero, Giovanni Micheli, and Sandro Carrara. «Fast synthesis of platinum nanopetals and nanospheres for highly-sensitive non-enzymatic detection of glucose and selective sensing of ions». In: *Scientific Reports* 5 (Oct. 2015), p. 15277. DOI: `10.1038/srep15277` (cit. on pp. 7, 14, 18).

[16] Andrzej Lewenstam. «Routines and Challenges in Clinical Application of Electrochemical Ion-Sensors». In: *Electroanalysis* 26 (June 2014). DOI: `10.1002/elan.201400061` (cit. on p. 8).

[17] Johan Bobacka. «Potential Stability of All-Solid-State Ion-Selective Electrodes Using Conducting Polymers as Ion-to-Electron Transducers». In: *Analytical chemistry* 71 (Nov. 1999), pp. 4932–7. DOI: `10.1021/ac990497z` (cit. on p. 9).

[18] Johan Bobacka, Mary McCarrick, Andrzej Lewenstam, and Ari Ivaska. «All-Solid-State Poly(Vinyl Chloride) Membrane Ion-Selective Electrodes with Poly(3-Octylthiophene) Solid Internal Contact». In: *Analyst* 119 (Sept. 1994). DOI: `10.1039/an9941901985` (cit. on p. 9).

[19] Francesca Criscuolo, Irene Taurino, Francesca Stradolini, Sandro Carrara, and Giovanni Micheli. «Highly-stable Li + ion-selective electrodes based on noble metal nanostructured layers as solid-contacts». In: *Analytica Chimica Acta* 1027 (May 2018). DOI: `10.1016/j.aca.2018.04.062` (cit. on pp. 10, 11, 14, 18, 37).

[20] Erno Lindner and Yoshio Umezawa. «Performance evaluation criteria for preparation and measurement of macro- and microfabricated ion-selective electrodes (IUPAC Technical Report)». In: *Pure and Applied Chemistry - PURE APPL CHEM* 80 (Jan. 2008), pp. 85–104. DOI: `10.1351/pac2008800 10085` (cit. on p. 13).

[21] Matthew Steinberg, Petar Kassal, and Ivana Steinberg. «System Architectures in Wearable Electrochemical Sensors». In: *Electroanalysis* 28 (Apr. 2016). DOI: `10.1002/elan.201600094` (cit. on p. 14).

[22] Rocio Canovas, Sara Sanchez, Marc Parrilla, María Cuartero, and Gaston Crespo. «Cytotoxicity Study of Ionophore-Based Membranes: Towards On-Body and In Vivo Ion Sensing». In: *ACS Sensors* 4 (Aug. 2019). DOI: `10.1021/acssensors.9b01322` (cit. on p. 14).

[23] Amay Bandodkar, Vinci Hung, Wenzhao Jia, Joshua Windmiller, Alexandra Martinez, Julian Ramírez, Garrett Chan, Kagan Kerman, and Joseph Wang. «Tattoo-based potentiometric ion-selective sensors for epidermal pH monitoring». In: *The Analyst* 138 (Oct. 2012). DOI: `10.1039/c2an36422k` (cit. on pp. 14, 15).

[24] Tomàs Guinovart, Amay Bandodkar, Joshua Windmiller, Francisco Andrade, and Joseph Wang. «A Potentiometric Tattoo Sensor for Monitoring Ammonium in Sweat». In: *The Analyst* 138 (Oct. 2013). DOI: `10.1039/c3an01672b` (cit. on pp. 14, 15).

[25] Marta Novell, Marc Parrilla, Gaston Crespo, and Francisco Andrade. «Paper-Based Ion-Selective Potentiometric Sensors». In: *Analytical chemistry* 84 (Apr. 2012), pp. 4695–702. DOI: `10.1021/ac202979j` (cit. on pp. 15, 27).

[26] Jinbo Hu, Andreas Stein, and Philippe Buhlmann. «A Disposable Planar Paper-Based Potentiometric Ion-Sensing Platform». In: *Angewandte Chemie International Edition* 55 (May 2016), pp. 7544–7547. DOI: 10.1002/anie.201603017 (cit. on p. 15).

[27] Wei Gao et al. «Fully integrated wearable sensor arrays for multiplexed in situ perspiration analysis». In: *Nature* 529 (Jan. 2016), pp. 509–514. DOI: 10.1038/nature16521 (cit. on pp. 16, 34, 37).

[28] Francesca Criscuolo, Ivan Ny Hanitra, Simone Aiassa, Irene Taurino, Nicolò Oliva, Sandro Carrara, and Giovanni Micheli. «Wearable multifunctional sweat-sensing system for efficient healthcare monitoring». In: *Sensors and Actuators B: Chemical* 328 (Feb. 2021), p. 129017. DOI: 10.1016/j.snb.2020.129017 (cit. on pp. 16, 37).

[29] R. Armstrong and M. Todd. «The role of PVC in ion selective electrode membranes». In: *Journal of Electroanalytical Chemistry - J ELECTROANAL CHEM* 237 (Nov. 1987), pp. 181–185. DOI: 10.1016/0022-0728(87)85231-2 (cit. on p. 20).

[30] Eric Bakker and Ernö Pretsch. «Potentiometric Sensors for Trace-Level Analysis». In: *Trends in analytical chemistry : TRAC* 24 (Apr. 2005), pp. 199–207. DOI: 10.1016/j.trac.2005.01.003 (cit. on p. 21).

[31] Tugba Kilic, Brunner Valerie, Laurent Audoly, and Sandro Carrara. «Smart e-Patch for drugs monitoring in schizophrenia». In: Dec. 2016, pp. 57–60. DOI: 10.1109/ICECS.2016.7841131 (cit. on p. 24).

[32] Tanji Yin, Dawei Pan, and Wei Qin. «All-Solid-State Polymeric Membrane Ion-Selective Miniaturized Electrodes Based on a Nanoporous Gold Film as Solid Contact». In: *Analytical chemistry* 86 (Oct. 2014). DOI: 10.1021/ac5029209 (cit. on p. 27).

[33] Katarzyna Wygl, Monika Durnaś, Pawel Parzuchowski, Zbigniew Brzózka, and Elżbieta Malinowska. «Miniaturized sodium-selective sensors based on silicon back-side contact structure with novel self-plasticizing ion-selective membranes». In: *Sensors and Actuators B-chemical - SENSOR ACTUATOR B-CHEM* 95 (Oct. 2003), pp. 366–372. DOI: 10.1016/S0925-4005(03)00440-4 (cit. on p. 28).

[34] Tanushree Ghosh, Hyun-joong Chung, and Jana Rieger. «All-Solid-State Sodium-Selective Electrode with a Solid Contact of Chitosan/Prussian Blue Nanocomposite». In: *Sensors* 2017 (Nov. 2017), p. 2536. DOI: 10.3390/s17112536 (cit. on p. 28).

[35] U Trebbe, M Niggemann, Karl Cammann, G Fiaccabrino, M Koudelka-Hep, Sergei Dzyadevych, and O Shulga. «A new calcium-sensor based on ion-selective conductometric microsensors - membranes and features». In: *Fresenius' journal of analytical chemistry* 371 (Dec. 2001), pp. 734–9. DOI: `10.1007/s002160101093` (cit. on p. 28).

[36] *Calcium Ionophore IV information sheet.* Merk KGaA. 2018 (cit. on p. 28).

[37] C. Dumschat, Michael Borchardt, C. Diekmann, J. Hepke, Karl Cammann, and M. Knoll. «Double matrix membranes for potentiometric cation selective disposable sensors». In: *Fresenius Journal of Analytical Chemistry* 348 (Aug. 1994), pp. 553–555. DOI: `10.1007/BF00323930` (cit. on p. 28).

[38] *Ammonium Ionophore I information sheet.* Merk KGaA. 2018 (cit. on p. 28).

[39] Dario Farina, Roberto Merletti, and Catherine Disselhorst-Klug. «Multi-Channel Techniques for Information Extraction from the Surface EMG». In: Jan. 2005, pp. 169–203. ISBN: 9780471678380. DOI: `10.1002/0471678384.ch7` (cit. on p. 32).

[40] NK Vøllestad. «Measurement of human muscle fatigue». In: *Journal of neuroscience methods* 74.2 (June 1997), pp. 219–227. ISSN: 0165-0270. DOI: `10.1016/s0165-0270(97)02251-6`. URL: `https://doi.org/10.1016/s0165-0270(97)02251-6` (cit. on p. 32).

[41] Leonard Bender. «Muscles Alive: Their Functions Revealed by Electromyography». In: *JAMA: The Journal of the American Medical Association* 201 (July 1967), p. 277. DOI: `10.1001/jama.1967.03130040073037` (cit. on p. 32).

[42] P. Bonato, S.H. Roy, M. Knaflitz, and C.J. de Luca. «Time-frequency parameters of the surface myoelectric signal for assessing muscle fatigue during cyclic dynamic contractions». In: *IEEE Transactions on Biomedical Engineering* 48.7 (2001), pp. 745–753. DOI: `10.1109/10.930899` (cit. on p. 33).

[43] B Bigland-Ritchie, E Donovan, and C Roussos. «Conduction Velocity and EMG Power Spectrum Changes in Fatigue of Sustained Maximal Efforts». In: *Journal of applied physiology: respiratory, environmental and exercise physiology* 51 (Dec. 1981), pp. 1300–5. DOI: `10.1152/jappl.1981.51.5.1300` (cit. on p. 33).

[44] Dario Farina, Roberto Merletti, Barbara Indino, Marco Nazzaro, and Marco Pozzo. «Surface EMG crosstalk between knee extensor muscles». In: *Muscle nerve* 26 (Nov. 2002), pp. 681–95. DOI: `10.1002/mus.10256` (cit. on p. 33).

[45] Mario Cifrek, Vladimir Medved, Stanko Tonkovic, and Sasa Ostojić. «Surface EMG Based Muscle Fatigue Evaluation in Biomechanics». In: *Clinical biomechanics (Bristol, Avon)* 24 (June 2009), pp. 327–40. DOI: `10.1016/j.clinbiomech.2009.01.010` (cit. on pp. 33, 35).

[46] Hermie Hermens, Bart Freriks, Catherine Disselhorst-Klug, and Günter Rau. «Development of recommendations for SEMG sensors and sensor placement procedures». In: *Journal of electromyography and kinesiology : official journal of the International Society of Electrophysiological Kinesiology* 10 (Oct. 2000), pp. 361–74. DOI: `10.1016/S1050-6411(00)00027-4` (cit. on p. 35).

[47] Miriam Gonzalez-Izal, Armando Malanda, Ion Navarro Amezqueta, E.M. Gorostiaga, F. Mallor, J Ibañez, and Mikel Izquierdo. «EMG spectral indices and muscle power fatigue during dynamic contractions». In: *Journal of electromyography and kinesiology : official journal of the International Society of Electrophysiological Kinesiology* 20 (May 2009), pp. 233–40. DOI: `10.1016/j.jelekin.2009.03.011` (cit. on p. 35).

[48] Ricardo Santos, Flavio Costa, Thais Saraiva, and Bianca Callegari. «Muscle fatigue in participants of indoor cycling». In: *Muscles, ligaments and tendons journal* 7 (May 2017), pp. 173–179. DOI: `10.11138/mltj/2017.7.1.173` (cit. on p. 35).